Pharmaceutical Research, Vol. 23, No. 4, April 2006 (© 2006)
DOI: 10.1007/s11095-006-9744-4

Research Paper

Molecular Mobility in Glass Forming Fananserine: A Dielectric, NMR, and TMDSC Investigation

L. Carpentier,[1,3] R. Decressain,[1] A. De Gusseme,[1] C. Neves,[2] and M. Descamps[1]

Received July 7, 2005; accepted December 13, 2005

Purpose. This study was conducted to characterize the molecular mobility of supercooled fananserine and derive from this analysis the non-Arrhenius and nonexponential properties of the primary α-relaxation.
Methods. The use of three investigation techniques of the molecular mobility, namely, dielectric relaxation, modulated differential scanning calorimetry, and proton nuclear magnetic resonance, allowed us to describe the dynamic properties of supercooled fananserine on a wide range of frequencies and temperatures, ranging from the melting temperature T_m = 372 K down to the glass transition temperature T_g = 292 K.
Results. We emphasized the capacity of these three techniques to give a coherent set of information. We used the coupling-model theory to interpret the dielectric results. It allowed us to identify two relaxation processes (α and β), corresponding to different molecular motions. The temperature evolution of the α-relaxation indicates that fananserine is a fragile glass former, as reflected by the steepness index value, m = 77. The temperature T_o where the relaxation times diverge was also determined.
Conclusions. The description of the dielectric relaxation data in terms of the Kohlrausch–Williams–Watt relaxation function has shown the existence of an additional low-amplitude relaxation process assigned to the so-called Johari–Goldstein process. Mainly concerned by the primary α-process directly involved in the glass formation, we derived from this analysis the characteristic features of this process and showed that supercooled fananserine is characterized by a strongly non-Arrhenius and nonexponential behavior.

KEY WORDS: α-relaxation; amorphous state; fragility; glass transition; nonexponential relaxation.

INTRODUCTION

Amorphous materials generally present a higher dissolution rate and solubility than their crystalline polymorphic forms. This can result in an increased bioavailability of amorphous drugs, which in turn improves their efficiency. However, amorphous materials are prone to recrystallization. Such phase transitions can occur during the manufacture or storage of the material and lead to unexpected modifications of its therapeutic properties. As a consequence, formulations involving stable crystalline forms are usually preferentially chosen, because it reduces the risk of uncontrolled phase transformations. However, if the formulation does contain an amorphous fraction, it is essential to evaluate its physical stability in time, to ensure that no structural modification can occur during the shelf life of the products. It requires the investigation of their molecular mobility, as the latter governs the structural modifications responsible for the phase transitions.

With regard to the stability of a given material, the glass transition temperature (T_g) is a fundamental parameter. Above T_g, the characteristic times are shorter than the timescale of the experiment, thus making structural rearrangements observable. These structural modifications are known as "primary" or α-relaxations. Any amorphous material should therefore be kept below T_g, to ensure that its dynamics is slow enough to prevent crystallization. However, this condition alone does not ensure physical stability in time. For example, it has been reported that amorphous indomethacin maintained 12°C below T_g recrystallized toward a stable crystalline form within a few weeks. When maintained 38°C below T_g, complete crystallization is achieved within 6 months (1). Also, Hancock *et al.* (2) showed that widely used compounds such as sucrose or polyvinylpyrrolidone (PVP) displayed a significant molecular mobility several tens of degrees below T_g, which potentially enables phase transitions in this temperature domain.

As a consequence, it is generally acknowledged that the ideal storage temperature of glassy materials should be below the Kauzmann temperature, T_K (3), at which the extrapolated entropy of the metastable liquid would be equal to that of the crystal. For a given material, T_K can be estimated from

[1] Laboratoire de Dynamique et Structures des Matériaux Moléculaires, UMR CNRS 8024, ERT 1018, Université de Lille 1, Bâtiment P5, 59655, Villeneuve d'Ascq Cedex, France.
[2] Analytical Sciences Department, Analytical Services, Sanofi Aventis, 13 quai Jules Guesdes, 94400 Vitry-sur-Seine, France.
[3] To whom correspondence should be addressed. (e-mail: laurent.carpentier@univ-lillel.fr)

the specific heat of the crystal and liquid phases. The storage of amorphous materials at $T < T_K$ normally ensures their physical stability for several months, or even years (4), because T_K can be identified to the temperature where the viscosity diverges as has been shown for many liquids (5).

In the viscous regime, the average structural α-relaxation time varies over more than 14 decades from the melting temperature (T_m) to the glass transition temperature T_g, where the viscosity attains 10^{13} Poise. This supercooled state of the liquid exhibits remarkable properties with regard to the temperature and time dependence of some transport coefficients and characteristic relaxation times (τ) that are often well approximated by the Vogel–Fulcher–Tamman (VFT) equation:

$$\tau(T) = \tau_0 \exp\left(\frac{A}{T - T_0}\right) \quad (1)$$

This relation implies a divergence of τ at a finite temperature T_0. The Arrhenius law obtained from Eq. (1) corresponds to the limit case where $T_0 = 0$ K. To compare and quantify the deviations from the thermally activated or Arrhenius behavior between different glass formers, a fragility or steepness index m has been introduced (6). It is defined as the slope of the characteristic relaxation times in a T_g-scaled Arrhenius diagram ($\log_{10}\tau$ *vs.* the reciprocal temperature). In other words, m measures how fast τ changes with T_g/T in the vicinity of the glass temperature T_g and is expressed as:

$$m = \left|\frac{d(\log_{10}\tau)}{d(T_g/T)}\right|_{T=T_g} \quad (2)$$

Moreover, the structural α-relaxation time does not usually decay exponentially as a function of time. Very often, the relaxation pattern follows the Kohlrausch–Williams–Watt (KWW) stretched exponential expression (7):

$$\phi(t) \propto \exp -\left(\frac{t}{\tau_{KWW}}\right)^{\beta_{KWW}} \quad (3)$$

The "stretching" exponent β_{KWW} ($0 < \beta_{KWW} \leq 1$) quantifies the deviation from the exponential decay. These different fundamental properties (non-Arrhenius and non-exponential behaviors) of glass-forming systems are highlighted in this paper on a pharmaceutical substance. Fananserine ($C_{23}H_{24}FN_3O_2S$) is a pharmaceutical active ingredient that possesses anxiolytic properties. It was first synthesized by Aventis-Pharma in the early 1990s (8). Fananserine is a complex molecule constituted of 54 atoms; it exhibits an important conformational flexibility, as shown in Fig. 1. Four polymorphs could be crystallized from solvent evaporation

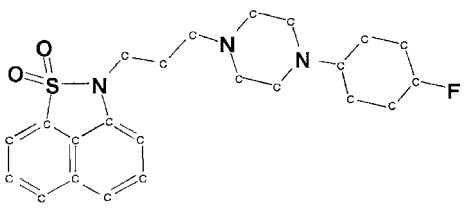

Fig. 1. Molecular structure of fananserine.

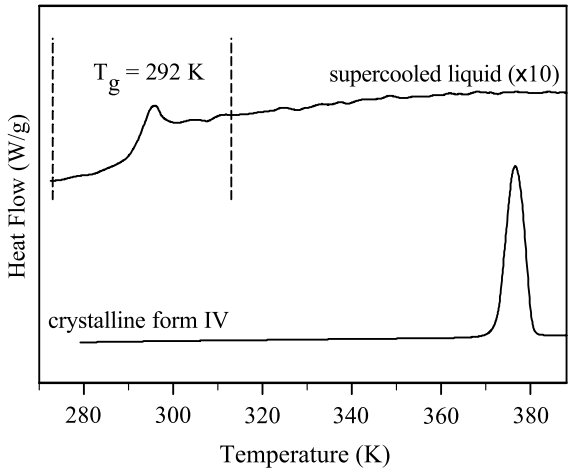

Fig. 2. Typical DSC thermograms obtained upon heating the crystalline IV phase and amorphous form of fananserine at a 5 K min^{-1} scanning rate. The temperature range between the two dashed lines localizes the temperature domain where the TMDSC experiments were carried out.

(9). They were numbered forms I to IV according to their chronological order of appearance, and their respective structures were resolved from X-ray powder diffraction patterns (10). The dynamic characterization presented here was carried out by dielectric, complex heat capacity, ^{1}H nuclear magnetic resonance (NMR) spin-lattice relaxation time measurements, on the supercooled liquid obtained from form IV, which is the most stable polymorph under ambient temperature and pressure.

MATERIAL AND METHODS

Material

Fananserine was obtained from Sanofi-Aventis (Paris, France) in its polymorphic form IV, and used as received. Form IV can be heated up to its melting point (T_m = 372 K) without undergoing any solid state transformation, as no enthalpic event can be observed in Fig. 2 prior to the melting point. Furthermore, differential scanning calorimetry (DSC) experiments (Fig. 2) show no sign of thermal degradation above T_m, which proves that fananserine is chemically stable when heated up to temperatures as high as T_m + 20 K. Liquid fananserine can be easily undercooled, without further cold crystallization. Upon heating at 5 K min^{-1}, the amorphous phase displays a glass transition at T_g = 292 K. Fananserine therefore exhibits two remarkable features with regard to its molecular mobility: an intrinsic conformational flexibility and a glass transition temperature close to ambient, making both the above and sub-T_g domains experimentally accessible.

Dielectric Spectroscopy Investigation

Isothermal measurements of the complex dielectric permittivity were performed with the analyzer DEA 2970 of TA instruments. It provides 7 decades of frequencies in the range 3 mHz–100 kHz), thus facilitating a complete assessment of the glass behavior [conventions usually fix the characteristic frequency $\nu(T_g) \cong 10$ mHz]. The dielectric cell

consists in an interdigitated array of electrodes on which the sample was melted, allowing an optimal filling of the cell. During the experiments the dielectric cell was protected against the room atmosphere and a dried airflow minimized hydration of the sample. A nitrogen cooling device provided testing capability from 120 to 700 K. In isothermal processes the temperature was controlled to within 0.01 K.

Thermal Analysis

Standard and temperature-modulated DSC (TMDSC) measurements were carried out using the MDSC 2920 of TA instruments in conjunction with a refrigerated cooling system (RCS). The calorimeter head was flushed with a highly pure helium gas. The baseline was calibrated by scanning the experimental temperature domain with an empty pan. The temperature and enthalpy readings were calibrated with respect to the melting point of pure indium. Fananserine was encapsulated in aluminum crimped pans. The sample weight, 10 mg, is low enough to ensure that the sample follows the imposed thermal oscillations. Isochronal measurements of the complex heat capacity $C^*_{p\omega}(T)$ were performed between 273 and 313 K (see Fig. 2 for the localization of this temperature domain with respect to T_g), using the following experimental parameters:

- Frequencies of the temperature modulation $\omega/2\pi$ ranging from 1/100 to 1/20 s^{-1}.
- Amplitudes A of the modulation chosen to keep the modu lated temperature rate constant for each experiment: $A\omega = \pi/100$ K s^{-1}.
- Low linear scanning rate $q = -0.1$ K min^{-1}, in order to limit "leveling effects" showing an artificial decrease in the am plitude of the imaginary part of $C^*_{p\omega}(T)$ when the frequency decreases (11). It also ensures that the con- ventional glass transition temperature T_g related to the linear rate q is clearly separated from the maximum loss temperature. In addition, it has been shown that for such low cooling rates, the data are reversible (11). $C^*_{p\omega}(T)$ thus corresponds to the heat capacity of the equilibrium metastable liquid. Finally, performing the measurements upon cooling allowed to avoid the enthalpy recovery effect, characteristic of annealed glasses.

NMR Analysis

^{1}H NMR experiments were performed on a Bruker ASX spectrometer operating at 100 MHz. The spin-lattice relaxation time T_{1z} was measured with the inversion recovery pulse sequence $(\pi, \tau, \pi/2, \text{Acq}, D_0)_n$ using 16–18 values of τ and a recycle delay $D_0 > 5T_{1z}$. Typical $\pi/2$ pulse lengths were 1.7 μs. The rotating frame spin-lattice relaxation time $T_{1\rho}$ was determined by locking the signal after a $\pi/2$ pulse with a $\pi/2$ phase-shifted field pulse and observing subsequent signal intensity as a function of the field pulse duration. A 17- and 8.4-G field pulse (B_1) was used. Over the temperature range studied, rapid spin diffusion resulted in an exponential decay of the magnetization that allowed us to define a single relaxation rate. The transversal relaxation time T_2 was determined by recording the free induction decay (FID) after a $\pi/2$ pulse and for short T_2 times by a solid echo pulse sequence. After Fourier transform of the FID, the spectral line width were determined and T_2 was obtained by using the relation: $\Delta\nu^{1/2} = 1/(\pi T_2)$. The sample used in NMR experiments was sealed under vacuum in glass tube. The temperature was controlled to within 1 K by a conventional gas flow system, and varied between 180 and 385 K. The precision of the NMR data obtained under such experimental conditions lies between ±5% for T_1 and ±15% for T_2 determination.

RESULTS AND DISCUSSION

Complex Dielectric Permittivity

After subtraction of the fitted conductivity contribution, the dielectric loss factor determined from 338 K down to 296 K, exhibits a pronounced peak associated to the primary α process, as shown in Fig. 3. The isothermal results were analyzed using the Havriliak–Negami (HN)-type dielectric permittivity expression:

$$\varepsilon^*(\omega) = \varepsilon_\infty + \frac{\varepsilon_s - \varepsilon_\infty}{(1 + (i\omega\tau_{HN})^\alpha)^\beta} \quad (4)$$

In Eq. (4), α and β characterize the symmetric and asymmetric broadening, respectively, (the limit case $\alpha = \beta = 1$ describes a Debye process corresponding to a monoexponential relaxation). The nonexponentiality quantified by these exponents α, $\beta < 1$ implies a distribution of the dielectric relaxation times. ε_∞ is the dielectric constant in

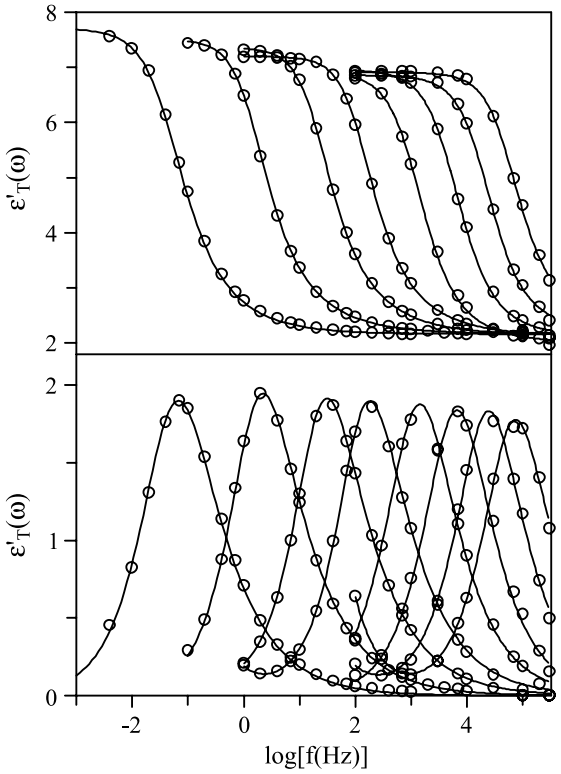

Fig. 3. Real $\varepsilon'_T(\omega)$ and imaginary $\varepsilon''_T(\omega)$ parts of the dielectric susceptibility of amorphous fananserine at various temperatures: the lowest temperature curve is recorded at 293 K, the other curves refer to a selection of isotherm recorded every 6 K up to 338 K in the order of increasing peak frequency. The solid lines result from fits with a Havriliak–Negami function.

the high-frequency limit and $\varepsilon = \varepsilon_s - \varepsilon_\infty$ is the relaxation strength with ε_s being the static dielectric constant. The parameters $\Delta\varepsilon$, τ_{HN}, α, and β for liquid fananserine were derived from the $\varepsilon''(\omega)$ data presented in Fig. 3. The broadening parameters increase from the low value 0.68 at 296 K to 0.82 at 338 K for β, and from 0.87 at 296 K to 0.92 at 338 K for α. As temperature rises, the $\varepsilon''(\omega)$ curves become narrower and more symmetrical, and their features get closer to those of a monoexponential relaxation, as the α and β values get closer to 1. This behavior is generally observed for metastable liquids: at high temperature, the motions related to the α process are weakly cooperative, and the distribution of the relaxation times in the amorphous state is relatively uniform. Lowering the temperature provokes an increase in viscosity and an increase in cooperativity. The distribution of the dielectric relaxation times broadens, resulting in a reduction of α and β. Although the temperature evolution of the broadening parameters gives global information on the primary relaxation, it does not allow to characterize precisely the nonexponential nature of the relaxations. Nevertheless, the refinements on a Havriliak–Negami function allowed us to determine the most probable relaxation time τ_{HN}, whose temperature dependence is clearly visible in an Arrhenius diagram (Fig. 7). This point will be further developed in the section "Arrhenius diagram."

Another method of dielectric data analysis consists in using the Fourier transform of the time response function $\phi(t)$ [Eq. (3)]. In this case, the number of variable parameters is smaller than for a refinement using the HN expression. This approach also presents the advantage of directly giving the characteristic time τ_{KWW} and also the coefficient $n = 1 - \beta_{\mathrm{KWW}}$ that reflects the physical features of the relaxations (7). Figure 4 shows the result of the refinements for the two temperatures closest to T_g, i.e., 296 and 302 K. They provide the following parameters:

$$-296\mathrm{K} : \tau_{\mathrm{KWW}} = 2s\,;\; n = 0.32$$
$$-302\mathrm{K} : \tau_{\mathrm{KWW}} = 0.14s\,;\; n = 0.30$$

The high-frequency wing of the α peak exhibits a decrease in slope (Fig. 4, dotted lines), where the KWW fit begins to fall bellow the experimental data. This "excess wing" is in fact related to an additional relaxation process corresponding to the so-called "Johari–Goldstein" (JG) secondary (or β) relaxation process (12). Although the microscopic processes governing this kind of β relaxations are still controversially discussed, they are admitted as being inherent to glass formers. Emerging from the α-relaxation in the supercooled domain, this process persists in the glassy state while assigning it an important residual molecular mobility. In the frequency domain, these two processes can either be distinctly separated, or the relaxation time τ_β associated to the JG relaxation can be close to the primary relaxation time τ_α. This situation is usually observed for small n values and also seems to be correlated to a low dielectric strength ε_β (13). In the present case, n is very low and the β peak is only perceivable in the flank of the predominating α peak by its high-frequency tail. The direct determination of the secondary relaxation times τ_β above T_g is therefore not possible for fananserine. The coupling model theory (14) formulated by K. L. Ngai, establishes a relation between the α-relaxation times and a primitive relaxation time τ_o, which is expected to be comparable to the τ_β of the JG relaxation (15):

$$\tau_o = (t_c)^n(\tau_\alpha)^{(1-n)} \tag{5}$$

where t_c, having the approximate value of 2×10^{-12} s for small molecular liquids, is a characteristic time of "crossover" separating the independent relaxations domain and the cooperative relaxations domain. The analysis of the dielectric data in the frame of the coupling model allowed us to localize the position in frequency of the JG-type sec- ondary relaxation. For fananserine, $\tau_0(296K) \approx \tau_\beta(296K) = 2.89.10^{-4}s$ and $\tau_0(302K) \approx \tau_\beta(302K) = 7.79.10^{-5}s$. The positions of τ are signaled in Fig. 4 by an arrow and reported in the Arrhenius diagram (Fig. 7).

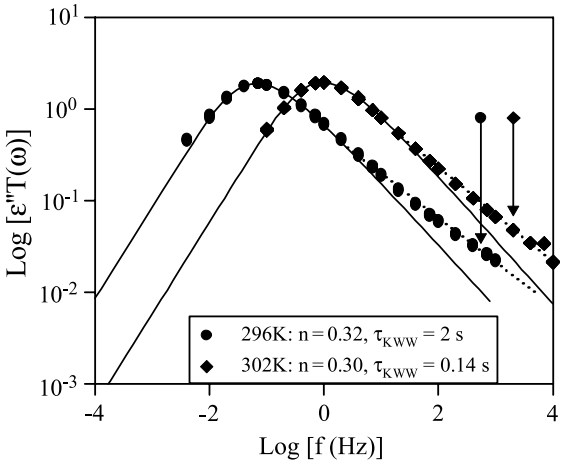

Fig. 4. The dielectric loss factor of fananserine at 296 and 302 K. The lines are KWW fits to the α-relaxation peaks with $n = 0.30$ (302 K) and $n = 0.32$ (296 K). Vertical arrows indicate the location of the relaxation peak calculated from relation (5).

Complex Heat Capacity

The TMDSC technique offers the possibility to explore a frequency domain ranging from 0.01 to 0.1 Hz. It therefore probes the enthalpic relaxation modes, which are also those observed in a conventional DSC scan. The theoretical basis and description of the TMDSC signals in terms of complex components of $C^*_{p\omega}(T)$ are described in detail in several articles, to which the reader may refer (11,16,17). Figure 5 shows the real and imaginary parts of the complex specific heat of liquid fananserine, as a function of inverse temperature, for each investigated frequency. The $C''_\omega(T)$ curves display peaks whose maxima climb at the temperature T_ω, where the real part $C'_\omega(T)$ drops. The $C'_\omega(T)$ and $C''_\omega(T)$ curves therefore exhibit the characteristic behavior of the complex susceptibility of a relaxation process. The temperature T_ω of the enthalpy loss maximum increases with ω. It corresponds to the temperature where the characteristic relaxation time of the sample $\tau(T_\omega) = 1/\omega$ is the most probable. The $C''_\omega(T)$ curve evolution indicates that the relaxation times in the liquid increase as T is lowered. Spectroscopic information about the activation energy and the (non)exponentiality of the relaxations can be deduced from these measurements.

The Arrhenius plot presented in Fig. 5b. gathers together the spectroscopic information obtained by specific

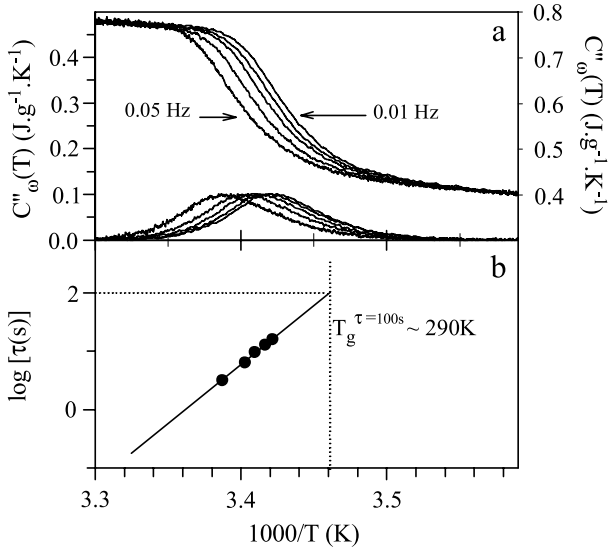

Fig. 5. (a) Real and imaginary parts of the complex heat capacity $C''_{p\omega}(T)$ as a function of reciprocal temperature at different frequencies in the range 0.01–0.05 Hz (linear cooling rate $q = -0.1$ K min^{-1}) for fananserine. (b) Enthalpic relaxation times are determined from the position of the $C''_{\omega}(T)$ maxima and are presented in a log scale as a function of the reciprocal temperature.

heat spectroscopy. As could be expected over such a narrow frequency/temperature domain, the evolution of the relaxation times follows an Arrhenius behavior:

$$\tau(T) = \tau_0 \exp\left(\frac{E}{RT}\right) \tag{6}$$

In this expression, the prefactor τ_0 is the characteristic relaxation time at infinite temperature and E is the activation energy. A fit of the experimental results to the above Arrhenius law yields $E = 390$ kJ mol^{-1} and $\tau_0 = 10^{-69}$ s. These values obviously have no direct physical meaning, but E can nevertheless be used to determine the steepness index (18,19).

TMDSC data are especially convenient for the determination of the steepness index of a glass-forming system. Localized on a narrow temperature domain, but just above the glass transition temperature, the Arrhenius evolution of the relaxation times allows us to define the steepness index by combining Eqs. (2) and (6):

$$m = \frac{E}{RT_g(\tau = 100\ s)\ln 10} \tag{7}$$

The glass transition temperature T_g, arbitrarily defined as $T(\tau = 100$ s), was deduced from the TMDSC experiments to be equal to 290 K. This result is consistent with the calorimetric T_g ($T_g = 292$ K), which shows that relaxation times measured by TMDSC spectroscopy can be attributed to the primary relaxation associated to the freezing out of the dynamic at the approach of T_g. It also attests to the reliability of the relaxation times measured by this technique. The determination of T_g enabled us to calculate m for fananserine using Eq. (7), from which we obtain $m = 70$. This high value of m attests to the fragile character of fananserine by comparison with the lower limit fragility ($m \cong 16$) for which the overall evolution of the dynamic follows an Arrhenius behavior. While operating in isochronal mode, the shape of the complex specific heat susceptibility $C^*_{p\omega}(T)$ allowed us to determine the stretching exponent β_{KWW} of relaxations, using the method proposed by Böhmer *et al.* (20). Applied to the 100 s curve, we obtained $\beta = 0.66$, which is consistent with the KWW exponent determined from the dielectric analysis.

NMR Spin-Lattice Relaxation Times

In NMR, the dynamics is monitored by measuring the spin-lattice relaxation $(T_{1z}, T_{1\rho})$and lineshape (T_2, $\Delta\upsilon_{1/2}$) evolution. The characterization of molecular motion is performed by comparing the temperature dependence of the relaxation rates. T_{1z} is associated with "rapid" motions (hundreds of MHz), whereas $T_{1\rho}$ probes "slow" motions on the frequency scale of the locking radio frequency (RF) field (B_1).

The experimental results are displayed in Fig. 6. In the vitreous state ($T < T_g$), a broad and almost Gaussian NMR spectrum is observed ($\Delta\upsilon_{1/2} \approx 34$ kHz). Such rigid-like band shape results from an important ^{1}H–^{1}H dipolar coupling. T_2 is constant down to $T = 156$ K, whereas a linear increase in spin-lattice relaxation rates $(T_{1z}, T_{1\rho})$ is observed with

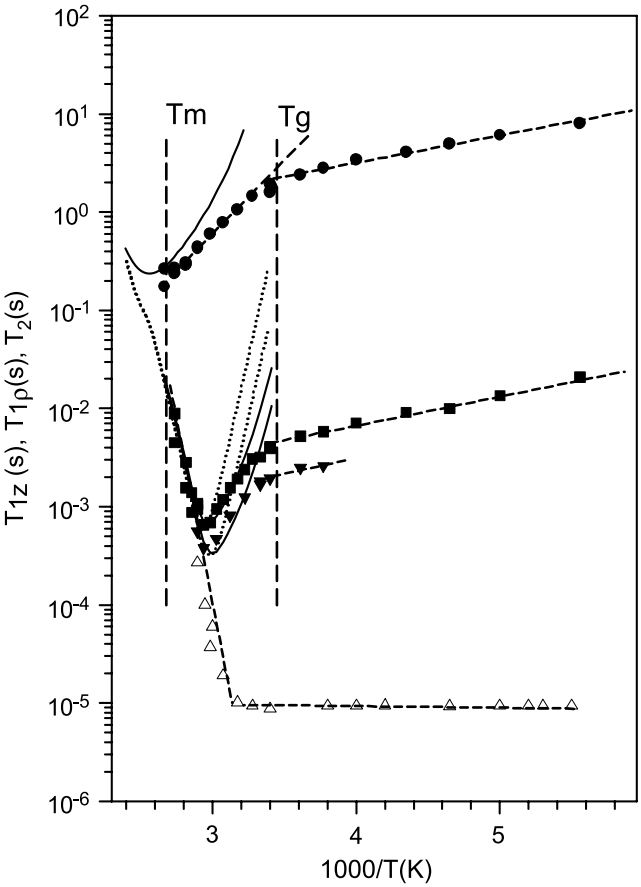

Fig. 6. Representation of proton T_{1z}(●), $T_{1\rho}$ (■: $B_1 = 17$ G, ▼: $B_1 = 8.4$ G), and T_2 (△) relaxation times as a function of temperature. The full and dotted lines correspond to the refinement of $T_{1\rho}$ using the HN function and the BPP model, respectively. Dashed lines are only a guide for eyes.

approximately the same activation energy: $E_A \approx 5.4$ kJ mol^{-1}. As the temperature increases, a motional line narrowing occurs just above T_g at $T \approx 322$ K. At this temperature the frequency of reorientations is of the same order of magnitude as the inverse experimental linewidth ($\tau \cong 3 \times 10^{-5}$ s). The glass transition T_g is related to an important change of slopes in the relaxation times variation. In the metastable domain ($T_g < T < T_m$), T_2 increases steadily up to T_m, where a sharp lineshape is observed. The T_{1z} measurements showed no minimum, but a linear decrease in the values of T_{1z} with increasing temperature. The slope gives an activation energy of $E_A \approx 33.28$ kJ mol^{-1}. The $T_{1\rho}$ measurements exhibit a minimum at $T = 340$ and 333 K for magnetic fields B_1 of 17 and 8.4 G, respectively. The slopes gave different activation energies above ($E_A \approx 124.8$ kJ mol^{-1}) and below ($E_A \approx 39.1$ kJ mol^{-1}) the minimum.

To extract the correlation time of molecular motions, a model description of the relaxation rates is necessary. It is well established that the NMR spin-lattice relaxation rates are proportional to a linear combination of spectral densities (21,22):

$$\frac{1}{T_{1z}} = C[J(\omega_0, \tau) + 4J(2\omega_0, \tau)] \tag{8}$$

$$\frac{1}{T_{1\rho}} = C\left[\frac{3}{2}J(2\omega_1, \tau) + \frac{5}{2}J(\omega_0, \tau) + J(2\omega_0, \tau)\right] \tag{9}$$

In Eqs. (8) and (9), $\omega_0 = \gamma B_0$ is the resonance angular frequency that depends on the gyromagnetic ratio γ of the nucleus and of the external field B_0, $\omega_1 = \gamma B_1$, with B_1 referring to the amplitude of the RF locking field, and τ is the correlation time of the molecular motion. Prefactor C is specific to the type of dominating spin coupling. When the relaxation is governed by dipolar interactions, C is expressed as (21,22):

$$C = \frac{2}{5}\left(\frac{\mu_0}{4\pi}\right)^2 \gamma^4 \hbar^2 \, I(I+1) \sum r^{-6} = \frac{2}{3}\gamma^2 M_2 \tag{10}$$

where I is the spin variable, and the summation over the internuclear distance r is taken over all the spins dipolarly coupled.

The first standard formalism of NMR relaxation analysis was developed by Bloembergem, Purcell, and Pound (BPP) (23). This high-field relaxation model [weak collisions theory (22)] assumes an isotropic rotational diffusion of the molecules leading to a monoexponential correlation function:

$$G(t) = \exp\left(-\frac{t}{\tau}\right)$$

The resulting spectral density $J(\omega)$ is a Lorentzian (or Debye) form:

$$J(\omega, \tau) = \frac{\tau}{1 + (\omega\tau)^2} \tag{11}$$

The BPP model predicts a minimum for the relaxation rates when $\omega_0\tau = 0.616(T_{1z})$ and $\omega_1\tau = 0.5(T_{1\rho})$, and a crossover from the rigid lattice limit (temperature-independent) to the motional region when $\Delta\omega\tau = 1$, where $\Delta\omega$ is the linewidth in the absence of motion. Because a minimum is observed for $T_{1\rho}$, we have determined a correlation time at the temperature of the $T_{1\rho}$ minima. The result, plotted as filled diamonds along with the dielectric data on the Arrhenius diagram (Fig. 7), shows that $T_{1\rho}$ is controlled by the α process observed by dielectric relaxation. Assuming an Arrhenius law [Eq. (6)] for the temperature dependence of the correlation times, we have applied the BPP model (Eq. (11)) to describe the $T_{1\rho}$ experimental data. As seen in Fig. 6, only a qualitative description was obtained with the parameters: $E_A = 124.8$ kJ mol^{-1}, $\tau_0 = 8\ 10^{-16}$s, and $M_2 = 4G^2(T_{1\rho})$. The discrepancy results from the existence of very different slopes of the curves $T_{1\rho} = f(10^3/T)$ above and below the minimum. The BPP model is unable to account for this dependence because it predicts identical E_a values. Similar behaviors are generally reported in NMR investigations of glassy materials (24). For glasses, it is generally admitted that the existence of different environments results in a non-Debye relaxation that cannot be described by a single correlation time τ. In such cases, a correlation time distribution has been introduced to describe the relaxation rates behavior. In the present work, the Havriliak–Negami

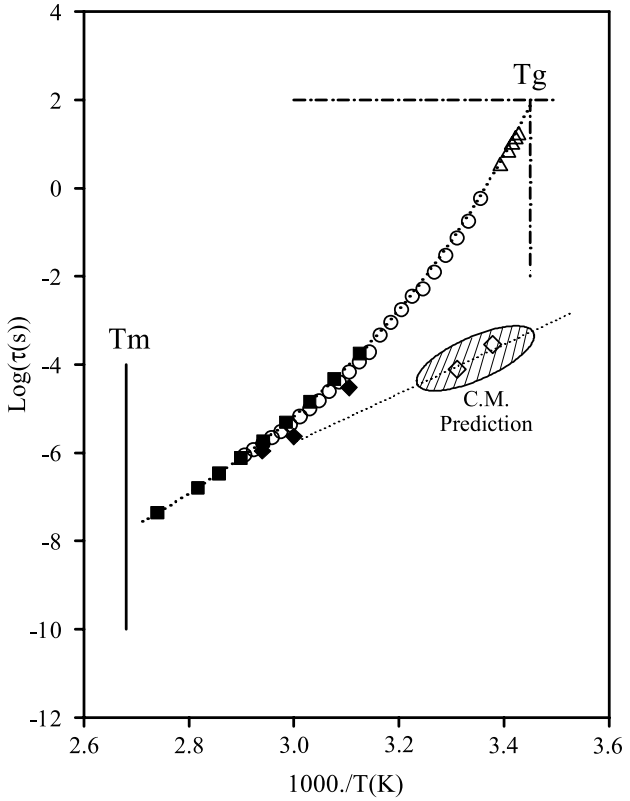

Fig. 7. Relaxation map for amorphous fananserine. △: Relaxation times determined by TMDSC; ○: relaxation times determined by dielectric measurements; ◆: ^{1}H NMR $T_{1\rho}$ minima and motional narrowing observed in T_2 evolution; ■: result from a fit of $T_{1\rho}$ with the HN function; ◊: relaxation times predicted by the coupling model and determined from relation (5).

(HN) relaxation function was used, giving the following equation for spectral density (25):

$$J_{HN}(\omega,\tau,\delta,\varepsilon) = \frac{1}{\omega}\sin\left[\varepsilon \arctan\left[\frac{(\omega\tau)^{\delta}\sin\left(\frac{\delta\pi}{2}\right)}{1+(\omega\tau)^{\delta}\cos\left(\frac{\delta\pi}{2}\right)}\right]\right] \times\left[1+(\omega\tau)^{2\delta}+2(\omega\tau)^{\delta}\cos\left(\frac{\delta\pi}{2}\right)\right]^{\left(-\frac{\varepsilon}{2}\right)} \quad (12)$$

In Eq. (12) δ is a parameter giving a measure of the degree of correlation between motions, and $\delta\varepsilon$ is a measure of the spread in height of the activation barrier of the motional process. δ ranges from 0 to 1, whereas ε ranges from 0 to $1/\delta$. The HN spectral density reduces to the Cole–Cole, Cole–Davidson, or BPP spectral density for $\varepsilon = 1$, $\delta = 1$, or $\varepsilon = \delta = 1$, respectively (25,26).

The *HN* function was used to simultaneously fit the experimental data around the temperature of the $T_{1\rho}$ minima ($T > T_g + 20$ K) by alternatively considering $T_{1\rho}$ first, then T_{1z}. Hence, doing the fitting procedure allows a rapid convergence of the $T_{1\rho}$ experimental data. Figure 6 shows that a satisfactory agreement can be obtained for $T > T_g + 20$ K, assuming a Vogel–Fulcher dependency of the correlation time [Eq. (1)]. The refined parameters are: $\tau_\alpha(t) = 5 \times 10^{-15}s$, $T_0 =$ 233 K, $E = 17.47$ kJ mol^{-1}, $\delta = 0.88$, $\varepsilon = 0.3$, and $M_2 = 8.5$ G^2. In the low temperature range ($T < T_g + 20$ K), the HN function failed to describe the experimental results. In this range, the $T_{1\rho}$ curves are probably not only determined by the α process, but also by the β process revealed by dielectric relaxation. Consequently, this result confirms the description of the dielectric loss factor in terms of two relaxational contributions. Moreover, when approaching T_g, and below the divergent temperature of the two processes, an important contribution to T_{1z} comes from the secondary relaxation not taken into account in our model. This certainly explained the observed discrepancy between T_{1z} and the *HN* model.

Arrhenius Diagram

The primary relaxation times for supercooled fananserine, obtained from the three different experimental approaches, are gathered together in Fig. 7. It clearly seems that the three techniques provide a coherent set of data with regard to the temperature dependence of τ. In particular, the results of TMDSC coherently prolong those of the dielectric spectroscopy in the close vicinity of T_g, revealing a good agreement between the relaxation times measured by the two techniques although they were obtained by applying different models. Dielectric, TMDSC, and NMR thus probe the same relaxation modes (dielectric, enthalpic, and spin-lattice), allowing—in the present case—a description of the molecular mobility on a wide range of frequencies/temperatures. The overall evolution of the primary process clearly shows a marked non-Arrhenius bending compatible with a Vogel–Fulcher–Tamman (VFT)-type behavior. The VFT expression is frequently adapted by replacing the parameter A in Eq. (1) by the product DT_0, where D is the "strength parameter" (6). The largest deviations from the Arrhenius law correspond to the smallest D values. The refinement of the Arrhenius diagram results in $D = 9.58$ and $T_0 = 232$ K for the temperature where relaxation times diverge. These values are very close to those obtained from the refinements achieved on the only NMR data of the spin-lattice relaxation times ($D = 9$; $T_0 = 233$ K). One can also notice that between the melting temperature and the glass transition temperature, the dynamics can be described solely by one VFT-type evolution, whereas for a number of glass-forming materials a VFT representation over a sufficiently large dynamic range generally requires separate low- and high-temperature VFT fits (27). As previously signaled, the glass forming materials are ordinarily classified and compared according to their steepness index m. Using the VFT expression in Eq. (2), m can be expressed in terms of the strength parameter D by:

$$m = \frac{DT_0T_g}{(T_g - T_0)^2}\log e \quad (13)$$

In this expression, the glass transition temperature T_g is associated to a relaxation time $\tau = 100$ s. Equation (13) gives $m = 77$ for fananserine. This value is close to the value determined from the TMDSC measurements by calculating the slope of the relaxation time at T_g. Taking into account the concordance of the stretching exponents β quoted above, this analysis confirms the capacity of TMDSC to give valuable information on the molecular mobility in a restricted temperature domain (one decade), but located close to T_g. Fananserine also conforms to the general trend that correlates the strong deviation from Arrhenius behavior ($m = 77$) to the nonexponential nature of the relaxations ($\beta_{KWW} =$ 0.66) (6).

CONCLUSION

The molecular mobility of amorphous fananserine has been characterized on a broad range of temperatures by dielectric analysis, TMDSC, and spin-lattice relaxation times measurements. It has been shown for fananserine that the dynamic characteristics obtained from these techniques were perfectly consistent, and allowed us to determine the parameters describing the non-Arrhenius and nonexponential features of this fragile glass former. The temperature at which the relaxation times diverge has been found to be $T_0 =$ 232 K, i.e., 60 K below T_g. Furthermore, the description of the dielectric relaxation data according to the KWW relaxation function has shown the existence of an additional low amplitude relaxation process assigned to the so-called Johari–Goldstein relaxation. Application of the coupling model has permitted the evaluation of the associated relaxation times. With respect to the stability of glasses, this secondary process could play a fundamental role. Indeed, some studies relate the occurrence of crystal nuclei in the glassy state to secondary relaxation processes (28,29). The characterization of molecular mobilities below T_g and their influences as precursor effects on the crystallization properties has to be addressed.

ACKNOWLEDGMENT

We gratefully acknowledge the financial support by the FEDER in the fame of an Interreg III program (Nord-Pas de Calais, Haute Normandie, Kent).

REFERENCES

1. M. Yoshioka, B. C. Hancock, and G. Zografi. Inhibition of indomethacin crystallization in poly(vinylpyrrolidone) coprecipitates. *J. Pharm. Sci.* **84**:983–986 (1995).
2. B. C. Hancock, S. L. Shamblin, and G. Zografi. Molecular mobility of pharmaceutical solids below the glass transition temperature. *Pharm. Res.* **12**:799–806 (1995).
3. M. D. Ediger, C. A. Angell, and S. R. Nagel. Supercooled liquids and glasses. *J. Phys. Chem.* **100**:13200–13212 (1996).
4. S. L. Shamblin, X. Tang, L. Chang, B. C. Hancock, and M. J. Pikal. Characterization of the time scales of molecular motion in pharmaceutically important glasses. *J. Phys. Chem., B.* **103**: 4113–4121 (1999).
5. H. Tanaka. Relation between thermodynamics and kinetics of glass-forming liquids. *Phys. Rev. Lett.* **90**:5701–5704 (2003).
6. R. Böhmer, K. L. Ngai, C. A. Angell, and D. J. Plazek. Nonexponential relaxations in strong and fragile glass formers. *J. Chem. Phys.* **99**:4201–4209 (1993).
7. J. C. Phillips. Stretched exponential relaxation in molecular and electronic glasses. *Rep. Prog. Phys.* **59**:1133–1207 (1996).
8. J. Giovannini. PhD thesis, University of Rennes 1, number 2648, 2001.
9. J. Giovannini, L. Ter Minassian, R. Ceolin, S. Toscani, M. A. Perrin, D. Louer, and F. Leveiller. Tetramorphism of fananserine: *p*, *T* diagram and stability hierarchy from crystal structure determinations and thermodynamic studies. *J. Phys., IV* **11**:123–126 (2001).
10. A. De Gusseme. PhD thesis, University of Lille 1, number 3353, 2003.
11. O. Bustin and M. Descamps. Slow structural relaxations of glass-forming Maltitol by modulated DSC calorimetry. *J. Chem. Phys.* **110**:10982–10992 (1999).
12. G. P. Johari. The glass transition and the nature of the glassy state. *Ann. N. Y. Acad. Sci.* **279**:117–140 (1976).
13. K. L. Ngai and M. Paluch. Classification of secondary relaxation in glass-formers based on dynamic properties. *J. Chem. Phys.* **120**:857–873 (2004).
14. K. L. Ngai. Relation between some secondary relaxations and the α relaxations in glass-forming materials according to the coupling model. *J. Chem. Phys.* **109**:6982–6994 (1998).
15. K. L. Ngai, P. Lunkenheimer, C. Leon, U. Schneider, R. Brand, and A. Loidl. Nature and properties of the Johari–Goldstein β-relaxation in the equilibrium liquid state of a class of glass-formers. *J. Chem. Phys.* **115**:1405–1413 (2001).
16. L. Carpentier, O. Bustin, and M. Descamps. Temperature-modulated differential scanning calorimetry as a specific heat spectroscopy. *J. Phys., D. Appl. Phys.* **35**:402–408 (2002).
17. S. Weyer, A. Hensel, and C. Schick. Phase angle correction for TMDSC in the glass-transition region. *Thermochim. Acta* **304–305**:267–275 (1997).
18. L. Carpentier, L. Bourgois, and M. Descamps. Contribution of temperature modulated DSC to the study of the molecular mobility in glass forming pharmaceutical systems. *J. Therm. Anal. Calorim.* **68**:727–739 (2002).
19. L. Carpentier, S. Desprez, and M. Descamps. From strong to fragile glass-forming systems: a temperature modulated differential scanning calorimetry investigation. *Phase Transit.* **76**:787–799 (2003).
20. R. Böhmer, E. Sanchez, and C. A. Angell. A.c. technique for simultaneous study of local and global linear responses near the glass transition: the case of doped calcium(2+)/potassium(1+)/nitrate. *J. Phys. Chem.* **96**:9089–9092 (1992).
21. A. Abragam. *Principles of Nuclear Magnetism*, Oxford University Press, Oxford, 1961.
22. C. P. Schlichter. *Principles of Magnetic Resonance,* 2nd ed. Springer, Heidelberg, 1978.
23. N. Bloembergen, E. M. Purcell, and R. V. Pound. Relaxation effects in nuclear magnetic resonance absorption. *Phys. Rev.* **73**:679–712 (1948).
24. R. Böhmer, G. Diezemann, G. Hinze, and E. Rössler. Dynamics of supercooled liquids and glassy solids. *Prog. Nucl. Magn. Reson. Spectrosc.* **39**:190–267 (2001).
25. P. A. Beckmann. Spectral densities and nuclear spin relaxation in solids. *Phys. Rep.* **171**:85–128 (1998).
26. C. Forte, M. Geppi, M. Malvaldi, and V. Mattoli. Dynamics of an amorphous polymer by an improved NMR approach based on the simultaneous analysis of ^{1}H and ^{13}C relaxation times. *J. Phys. Chem., B.* **108**:10832–10837 (2004).
27. F. Stickel, E. W. Fischer, and R. Richert. Dynamics of glass-forming liquids. II. Detailed comparison of dielectric relaxation, dc-conductivity, and viscosity data. *J. Chem. Phys.* **104**: 2043–2055 (1996).
28. N. Okamoto, M. Oguni, and Y. Sagawa. Generation and extinction of a crystal nucleus below the glass transition temperature. *J. Phys. Condens. Matter* **9**:9187–9198 (1997).
29. M. Hatase, M. Hayana, T. Hikima, and M. Oguni. Discovery of homogeneous-nucleation based crystallization in simple glass-forming liquid of toluene below its glass-transition temperature. *J. Non-Cryst. Solids* **307–310**:257–263 (2002).